JOURNAL OF AGRICULTURAL AND FOOD CHEMISTRY

Article

pubs.acs.org/JAFC

Metabolic Effect of an Exogenous Gene on Transgenic *Beauveria bassiana* Using Liquid Chromatography−Mass Spectrometry-Based Metabolomics

Feifei Luo,[†] Ruili Lu,[†] Hong Zhou,[‡] Fenglin Hu,*[,†] Guanhu Bao,[†] Bo Huang,[†] and Zengzhi Li[†]

[†]Research Center on Entomogenous Fungi, Anhui Agricultural University, Hefei, 230036 Anhui, People's Republic of China

[‡]Department of Applied Mathematics, Naval Postgraduate School, Monterey, California 93943, United States

ABSTRACT: Genetic modification of *Beauveria bassiana* with the scorpion neurotoxin *aaIT* gene can distinctly increase its insecticidal activity, whereas the effect of this exogenous gene on the metabolism of *B. bassiana* is unknown until now. Thus, we investigate the global metabolic profiling of mycelia and conidia of transgenic and wild-type *B. bassiana* by liquid chromatography−mass spectrometry (LC−MS). Principal component analysis (PCA) and orthogonal projection to latent structure discriminant analysis (OPLS-DA) reveal clear discrimination of wild-type mycelia and conidia from transgenic mycelia and conidia. The decrease of glycerophospholipids, carnitine, and fatty acids and the increase of oxylipins, glyoxylate, pyruvic acid, acetylcarnitine, fumarate, ergothioneine, and trehalose in transgenic mycelia indicate the enhanced oxidative reactions. In contrast, most metabolites related to oxidative stress are not altered significantly in conidia, which implies that there will be no significant oxidative stress reaction when the *aaIT* gene is quiescent in cells.

KEYWORDS: *B. bassiana, transgenic strains, metabolomics, LC−MS, glycerophospholipid, oxidative stress, metabolic pathway, antioxidant*

1. INTRODUCTION

Environmental problems of chemical insecticides have stimulated efforts to employ biological control agents. However, only few alternative products have been widely used to control pests, despite their promising potentials. The failed reasons have included slow kill, failure to identify strains active at low doses, and inconsistent control effects compared to chemical insecticides.[1] Hitherto, at least 12 species or subspecies (varieties) of entomogenous fungi have been employed and registered as mycoinsecticides and mycoacaricides.[2] *Beauveria* and *Metarhizium* are most commonly used for biological control because their conidia are relatively easy and inexpensive for mass production in field applications.[3] The utility of a genetic engineering technique to introduce an exogenous gene can markedly increase the virulence of entomopathogenic fungi.[3,4] Recently, most research on the virulence of entomogenous fungi has focused on the genes of lipase, chitinase, protease, etc. Furthermore, the scorpion neurotoxin from the buthid scorpion *Androctonus australisis* is widely applied in transgenic biological pesticides because of its strict selectivity for insects and higher safety for mammals.[5,6]

B. bassiana was transformed with scorpion neurotoxin *aaIT* gene by our research group and co-workers, and in comparison to the wild-type strain, the engineered isolates take fewer spores to kill 50% of pine caterpillars than the wild type.[7] However, it is unclear how the metabolites of *B. bassiana* are influenced by the *aaIT* gene. Results of this study will not only contribute to the chemeco-safety study of transgenic fungi but also reveal the regulative mechanism of an exogenous gene on cell metabolisms. Various metabolisms are linked to each other in a complex biological system, and there is increasing evidence that indicates that artificial alteration in gene expression may lead to the changes of many other metabolisms.[8−12] A metabolomic approach that is a complementary technology to genomics and proteomics is required to reveal this effect. To the best of our knowledge, there is no metabolomic report on the transgenic fungus.

The goal of this work is to distinguish different metabolites of mycelia and conidia from transformant and wild-type *B. bassiana* using high-performance liquid chromatography−time-of-flight−mass spectrometry (HPLC−TOF−MS) coupled with multivariate analysis. In addition, analysis of the metabolic pathway in which these biomarkers participate can reveal the metabolic perturbation of the *aaIT* gene on wild-type *B. bassiana*.

2. MATERIALS AND METHODS

2.1. Chemicals and Reagents. HPLC-grade acetonitrile was purchased from Merck (Germany). Formic acid was of HPLC grade and was purchased from Agilent (Santa Clara, CA). Deionized water was prepared using a water purification system (Millipore, Billerica, MA). All other reagents used in this study were of analytical grade.

2.2. Fungal Strain and Maintenance. *B. bassiana aaIT* single transgenic strains Bb13T-10-3 and Bb13T-4-1 and wild-type strain Bb13 have been catalogued and deposited in the Research Center on Entomogenous Fungi (Hefei, China).[7] The strains are preserved as mycelial pieces on agar slants at 4 °C, in distilled water at room temperature, in sterile 10% aqueous glycerol in liquid nitrogen, and as spores in milk sealed in a glass tube after freeze-drying, which are stored at 4 °C.

2.3. Fungal Culture and Workup. Fungal isolates were cultured on potato dextrose agar (PDA) medium (200 g/L potato, 20 g/L glucose, and 20 g/L agar) at 25 °C for 15 days. The conidia were

Received: April 17, 2013
Revised: June 17, 2013
Accepted: June 19, 2013
Published: June 19, 2013

dx.doi.org/10.1021/jf401703b | J. Agric. Food Chem. 2013, 61, 7008−7017

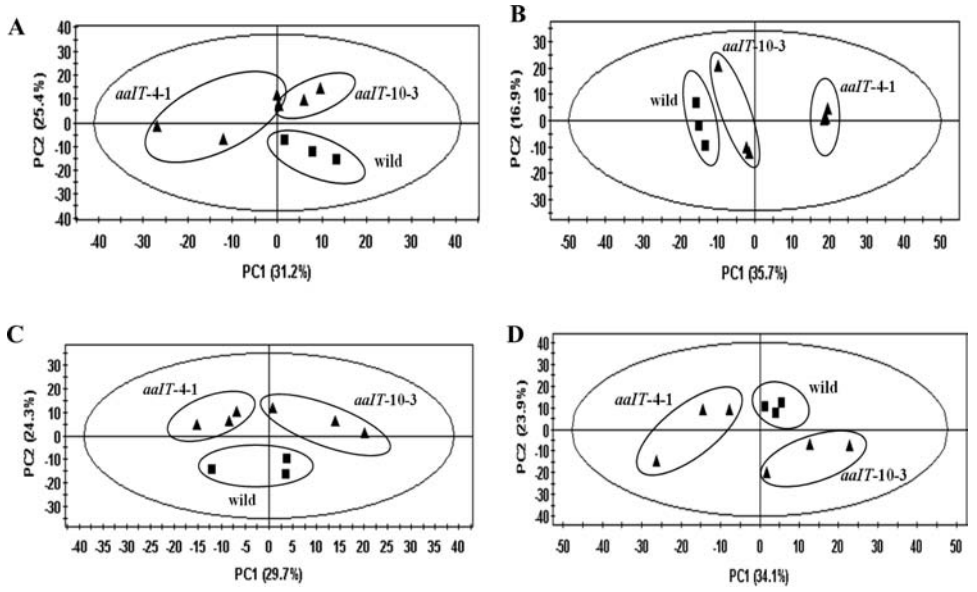

Figure 1. PCA score plots derived from HPLC−MS spectra of (A) mycelia and (B) conidia extracts in positive mode and (C) mycelia and (D) conidia extracts in negative mode: (■) wild type and (▲) transformant.

flooded with an aqueous solution of 0.01% Tween 80 and filtered through sterile absorbent cotton. The final spore concentration was adjusted to 1×10^6 spores/mL. The surspension was inoculated 200 μL/dish on cellophane membrane precovered PDA plates and cultured at 25 °C.

Mycelia were harvested at 5 days of growth by a scoop, transferred to 5 mL centrifuge tubes, subsequently frozen in liquid nitrogen, and kept at −80 °C. Spores were collected at 15 days post-inoculation by scrapping the colony into 40 mL of 0.01% Tween 80 solution, and the contents were vortexed and filtered through a 20 μm filter cloth. The filtrate was transferred to a 50 mL centrifuge tube and centrifuged for 10 min at 8000 revolutions/min. The precipitate was suspended in 2 mL of distilled water and transferred to a 5 mL centrifuge tube; then the spore suspension was centrifuged for 10 min at 10 000 revolutions/min; and, finally, the conidia were kept at −80 °C. All samples were collected in three biological replicates. Mycelia and conidia were lyophilized for 48 h, and mycelia were crushed into a fine powder and then kept at 4 °C until extraction. The lyophilized powder (mycelium or conidium) was weighed, and 10 mg of sample was extracted with 2 mL of 80% MeOH, followed by 1 min of vortexing and subsequent sonication for 1 h. Samples were further kept at 4 °C for 12 h in the dark. After centrifugation at 10 000 revolutions/min for 10 min, 1.8 mL of supernatant was collected and dried with a centrifugal concentrator. All samples were stored at −80 °C until analysis. The dried extracts were redissolved ultrasonically in 300 μL of 90% methanol and filtered through a 0.22 μm polyvinylidene fluoride (PVDF) membrane filter before HPLC−MS analysis.

2.4. LC−MS Data Acquisition. The chemical compositions of mycelia and conidia extracts were analyzed using an Agilent 1100 HPLC with a photodiode array detector (PAD) coupled to a 6210 TOF mass spectrometer with an electrospray ionization (ESI) source. The chromatographic separation was performed on an Agilent Eclipse XDB-C18 (5 μm, 150 × 2.1 mm inner diameter), and the LC parameters were as follows: injection volume, 5 μL; column temperature, 40 °C; flow rate, 0.3 mL/min; and the eluates were monitored with a PAD at full-length scan from 200 to 600 nm. The mobile phase was (A) 0.1% formic acid in water and (B) 0.1% formic acid in acetonitrile, and gradient elution was carried out: 5% B for 0−3 min, 5−100% B for 3−50 min, and 100% B for 50−60 min. The column was reconditioned with an initial gradient for 12 min. The mass spectrometer parameter settings used for the measurement were as follows: ionization mode, positive and negative; gas temperature, 350 °C; drying gas, 12 L/min; nebulizer pressure, 45 psi; capillary voltage, 4000 V in positive mode and 3500 V in negative mode; fragmentor voltage, 215 V in positive mode and 170 V in negative mode; skimmer voltage, 60 V; and OCT 1 RF, 250 V. Data acquisition was performed in the m/z range of 50−1100 Da.

2.5. Data Processing and Statistical Analysis. The raw data from LC−TOF chromatograms were preprocessed by MassHunter software (Agilent Technologies, Santa Clara, CA) using the molecular feature extraction (MFE) algorithm for automated peak detection and chromatographic deconvolution. Peaks with signal-to-noise (S/N) ratios lower than 5 were rejected. The mass/retention time/peak height data array for each sample were generated and exported as a .csv file. Then, all of the data were uploaded to MetaboAnalyst for subsequent data process and statistical analysis.[13,14] Peaks were aligned across all samples using the parameters of 0.01 Da and 0.5 min tolerance. Finally, the processed data were downloaded for multivariate analysis. Principal component analysis (PCA) and orthogonal projection to latent structure discriminant analysis (OPLS-DA) were performed by SIMCA-P+ (version 12.0, Umetrics, Umea, Sweden). The intensity for each peak was normalized to the sum of the peak intensities for each data set,[15,16] and pareto scaling was applied for PCA and OPLS-DA. One-way analysis of variation (ANOVA), t test, and hierarchical clustering analysis (HCA) were carried out by MetaboAnalyst. The metabolic pathway was referred to the KEGG database.[17]

2.6. Metabolite Identification. Metabolite identification was performed in the following approaches: (1) The molecular formula calculated by the MassHunter software based on the accurate mass and isotopic pattern recognitions was used for confirming putative identities by searching against the in-house database of entomopathogenic fungi and web databases [Dictionary of Natural Products (DNP, Chapman & Hall/CRC), METLIN, PUBCHEM, and CHEMSPIDER]. (2) The fragments of the metabolite were compared to the compounds that have the same or similar configuration in METLIN and MASSBANK. (3) Putative biomarkers were verified by its elution order (polarity) and structure characteristics. (4) The ultraviolet/visible (UV/vis) spectra were used in the identification whenever possible. (5) The ambiguous metabolites were identified by comparison to authentic compounds available and/or referring to the published literature about fungi, especially entomopathogenic fungi.

3. RESULTS AND DISCUSSION

3.1. Multivariate Analysis. LC−MS coupled with multivariate statistical analysis was used to study the metabolomic differences of mycelia and conidia extracts from transgenic

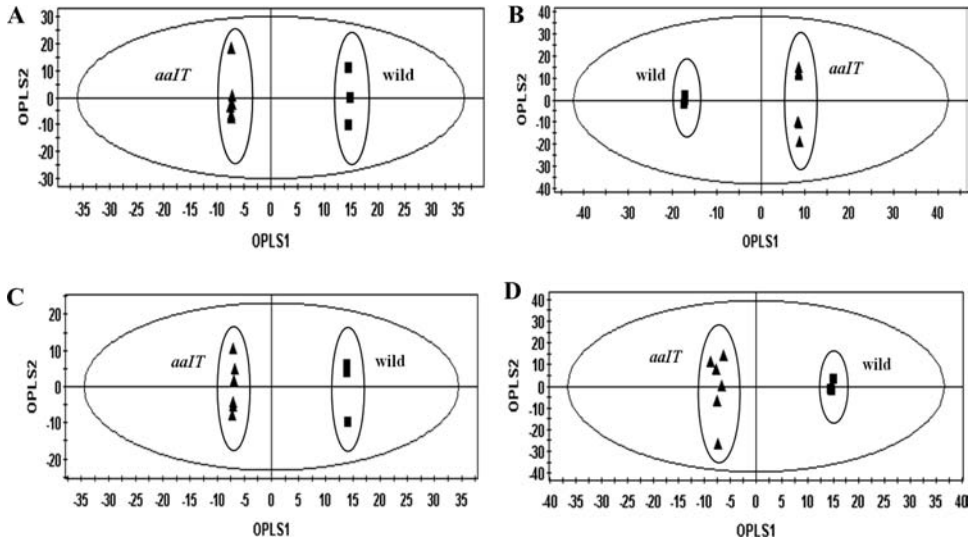

Figure 2. OPLS-DA score plots derived from HPLC−MS spectra of (A) mycelia (R^2X = 0.75, R^2Y = 0.99, and Q^2 = 0.89) and (B) conidia (R^2X = 0.69, R^2Y = 0.99, and Q^2 = 0.91) extracts in positive mode and (C) mycelia (R^2X = 0.79, R^2Y = 0.99, and Q^2 = 0.95) and (D) conidia (R^2X = 0.81, R^2Y = 0.99, and Q^2 = 0.81) extracts in negative mode: (■) wild type and (▲) transformant.

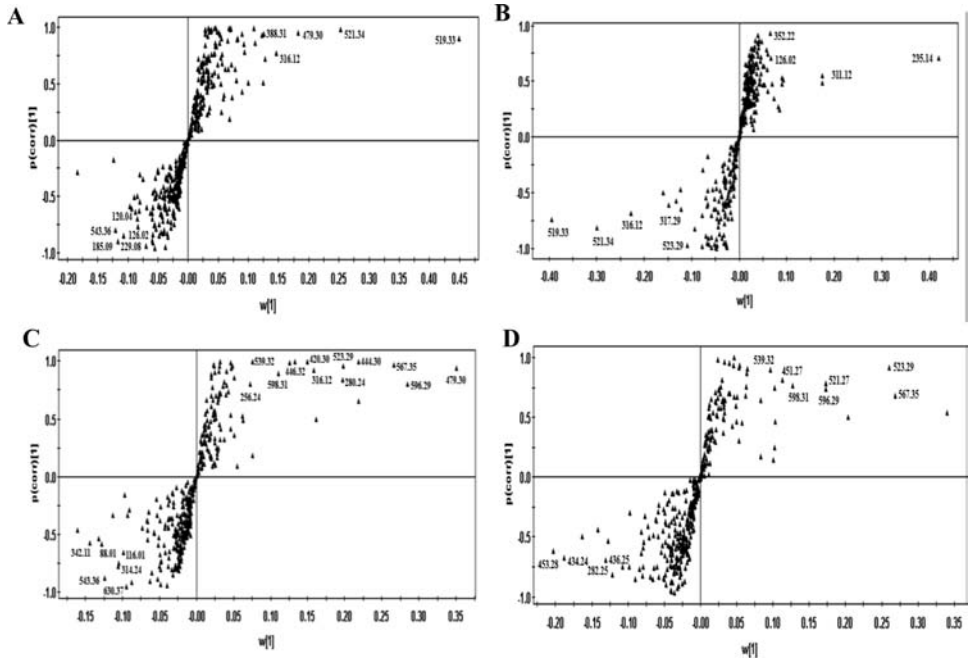

Figure 3. S plots generated from OPLS-DA models of (A) mycelia and (B) conidia extracts in positive mode and (C) mycelia and (D) conidia extracts in negative mode. The metabolites of mycelia and conidia extracts are identified in Tables 1 and 2, respectively.

(Bb13T-10-3 and Bb13T-4-1) and wild-type (Bb13) *B. bassiana*. PCA, an unsupervised pattern recognition method, is initially performed to examine intrinsic variation in the data set. A score plot is applied for the grouping of samples by reducing the dimensionality of the data. The data sets exhibiting similarities are clustered together, and those that are different are placed further apart.[18]

As shown in Figure 1, PCA score plots of mycelia and conidia samples employed in this study found that the two single transgenic isolates were clearly separated from the wild-type isolate. It is evident that the metabolisms of mycelia and conidia are strongly affected by the *aaIT* gene. However, Bb13T-10-3 and Bb13T-4-1 were not clustered into one group, and Bb13T-10-3 was closer to the wild type in the conidia samples in positive mode (Figure 1B). The significant features of transgenic and wild-type strains were not easy to identify by the corresponding loading plots (data not shown). Although PCA is undoubtedly a reliable grouping method in metabolomics, if variation within the sample of the same group is bigger than between groups, a clear separation of each group cannot be expected because the separation of PCA is achieved from unbiased maximum variation within the samples tested.[19] Therefore, a supervised pattern recognition method OPLS-DA was used to maximize the separation between the groups and discriminate differential metabolites of engineered and wild-type strains. OPLS-DA helps the screening of marker metabolites

Table 1. Metabolites Putatively Identified by HPLC−TOF−MS in Mycelia Extracts

RT (min)	detected mass	metabolite[a]	ionization mode	molecular formula	theoretical mass	Δmass (mDa)	change[b]
1.28	74.00040	glyoxylate	ESI(−)	$C_2H_2O_3$	74.00039	−0.01	↑
1.96	88.01640	pyruvic acid	ESI(−)	$C_3H_4O_3$	88.01604	−0.36	↑
1.28	116.01080	fumarate	ESI(−)	$C_4H_4O_4$	116.01096	0.16	↑
1.26	117.07913	betaine	ESI(+)	$C_5H_{11}NO_2$	117.07898	−0.15	↓
1.46	120.04360	purine	ESI(+)	$C_5H_4N_4$	120.04360	0.00	↑
1.32	126.02548	2-methylsulfanylpyrimidine	ESI(+)	$C_5H_6N_2S$	126.02517	−0.31	↑
1.23	150.05268	ribulose	ESI(−)	$C_5H_{10}O_5$	150.05282	0.14	↓
1.23	161.10553	carnitine	ESI(+)	$C_7H_{15}NO_3$	161.10519	−0.34	↓
1.35	185.09815	5-hexyl-1,3,4-thiadiazol-2-amine	ESI(+)	$C_8H_{15}N_3S$	185.09867	0.52	↑
1.33	203.11581	acetylcarnitine	ESI(+)	$C_9H_{17}NO_4$	203.11576	−0.01	↑
1.33	229.08846	ergothioneine	ESI(+)	$C_9H_{15}N_3O_2S$	229.08850	0.04	↑
48.37	256.24061	palmitic acid	ESI(−)	$C_{16}H_{32}O_2$	256.24023	−0.38	↓
1.31	257.10367	glycerophosphocholine	ESI(+)	$C_8H_{20}NO_6P$	257.10280	−0.87	↓
46.31	280.24067	linoleic acid	ESI(−)	$C_{18}H_{32}O_2$	280.24023	−0.44	↓
1.17	295.05885	5-aminoimidazole ribonucleotide	ESI(+)	$C_8H_{14}N_3O_7P$	295.05694	−1.91	↓
36.90	296.23574	8-hydroxy-linoleic acid	ESI(−)	$C_{18}H_{32}O_3$	296.23514	−0.60	↑
46.55	306.25650	linolenic acid ethyl ester	ESI(+)	$C_{20}H_{34}O_2$	306.25590	−0.60	↓
49.46	308.27174	linoleic acid ethyl ester	ESI(+)	$C_{20}H_{36}O_2$	308.27150	−0.24	↓
32.00	314.24591	7,8-dihydroxy-oleic acid	ESI(−)	$C_{18}H_{34}O_4$	314.24571	−0.20	↑
1.48	316.12692	mycosporin glutamicol; 5′-carboxylic acid, 1′-amide	ESI(+) and ESI(−)	$C_{13}H_{20}N_2O_7$	316.12705	0.13	↓
34.95	338.28198	2-hydroxy-5,9-eicosadienoic acid; (2*ξ*,5*Z*,9*Z*)-form, Me ether	ESI(+)	$C_{21}H_{38}O_3$	338.28210	0.12	↓
1.24	342.11617	trehalose	ESI(−)	$C_{12}H_{22}O_{11}$	342.11621	0.04	↑
48.83	388.31932	1-heptadecene-4,6,8,10,12-pentol; (4*S*,6*S*,8*R*,10*R*,12*R*)-form,penta-Me ether	ESI(+)	$C_{22}H_{44}O_5$	388.31887	−0.45	↓
46.55	412.31907	chondrillin	ESI(+)	$C_{24}H_{44}O_5$	412.31887	−0.20	↓
49.48	414.33454	tetrahydro-2,3,5-trihydroxy-6-nonadecyl-4*H*-pyran-4-one	ESI(+)	$C_{24}H_{46}O_5$	414.33452	−0.02	↓
39.73	420.30935	1-hexadecanoyl glucitol	ESI(−)	$C_{22}H_{44}O_7$	420.30870	−0.65	↓
38.09	444.30892	citric acid; 2-octadecyl ester	ESI(−)	$C_{24}H_{44}O_7$	444.30870	−0.22	↓
40.90	446.32505	mono-9-octadecenoyl glucitol	ESI(−)	$C_{24}H_{46}O_7$	446.32435	−0.70	↓
32.78	477.28499	PE(18:2/0:0)	ESI(+) and ESI(−)	$C_{23}H_{44}NO_7P$	477.28554	0.55	↓
35.12	479.30060	PE(18:1/0:0)	ESI(+) and ESI(−)	$C_{23}H_{46}NO_7P$	479.30119	0.59	↓
32.04	493.31640	PC(16:1/0:0)	ESI(+)	$C_{24}H_{48}NO_7P$	493.31684	0.44	↓
31.80	517.31703	PC(18:3/0:0)	ESI(+)	$C_{26}H_{48}NO_7P$	517.31684	−0.19	↓
33.17	519.33192	PC(18:2/0:0)	ESI(+)	$C_{26}H_{50}NO_7P$	519.33249	0.57	↓
34.88	521.27549	PS(18:2/0:0)	ESI(−)	$C_{24}H_{44}NO_9P$	521.27537	−0.12	↓
35.82	521.34751	PC(18:1/0:0)	ESI(+)	$C_{26}H_{52}NO_7P$	521.34814	0.63	↓
36.67	523.29086	PS(18:1/0:0)	ESI(+) and ESI(−)	$C_{24}H_{46}NO_9P$	523.29102	0.16	↓
33.37	539.32300	PS(19:0/0:0)	ESI(−)	$C_{25}H_{50}NO_9P$	539.32232	−0.68	↓
41.44	543.36688	beauverolide B	ESI(+) and ESI(−)	$C_{31}H_{49}N_3O_5$	543.36722	0.34	↑
36.91	567.35389	PS(21:0/0:0)	ESI(−)	$C_{27}H_{54}NO_9P$	567.35362	−0.27	↓
43.16	591.36763	beauverolide C	ESI(−)	$C_{35}H_{49}N_3O_5$	591.36722	−0.41	↑
34.90	596.29639	PI(18:2/0:0)	ESI(−)	$C_{27}H_{49}O_{12}P$	596.29616	−0.23	↓
37.80	598.31236	PI(18:1/0:0)	ESI(−)	$C_{27}H_{51}O_{12}P$	598.31181	−0.55	↓
41.77	630.37860	beauverolide Ka	ESI(+) and ESI(−)	$C_{37}H_{50}N_4O_5$	630.37812	0.48	↑

[a]Abbreviations: PE, phosphatidylethanolamine; PC, phosphotidylcholine; PS, phosphatidyserine; and PI, phosphatidylinositol. [b]Relative metabolite level in mycelia of transgenic strains in comparison to the wild-type strain (↑, increase; ↓, decrease).

responsible for maximum separation by removing systematic variation unrelated to grouping.

As Figure 2 showed, OPLS-DA between transgenic and wild-type *B. bassiana* samples was implemented to investigate the metabolic influences of the *aaIT* gene on the wild-type strain. Clear separation according to the first component (OPLS1) was observed in the score plots. The OPLS-DA models of mycelia and conidia were established using one predictive and three orthogonal components. Subsequently, the S plots from the OPLS-DA models were constructed to understand the metabolites responsible for the differentiation (Figure 3). The lower left quadrant of the S plot displays the higher levels of metabolites in the left group related to the right group in the OPLS-DA score plot, whereas those placed in the higher right quadrant show the higher levels of metabolites in the right group. The S plot shows the covariance p against the correlation $p(\mathrm{corr})$ of the variables of the discriminating component of the OPLS-DA model. Cutoff values for the covariance of $p \geq |0.05|$ and for the correlation of $p(\mathrm{corr}) \geq |0.5|$ were used. Moreover, the significances of the discriminatory metabolites were confirmed by a pairwise comparison to the t test.

Table 2. Metabolites Putatively Identified by HPLC−TOF−MS in Conidia Extracts

RT (min)	detected mass	metabolite[a]	ionization mode	molecular formula	theoretical mass	Δmass (mDa)	change[b]
2.37	100.01609	succinic anhydride	ESI(−)	$C_4H_4O_3$	100.01604	−0.05	↓
1.32	126.02548	2-methylsulfanylpyrimidine	ESI(+)	$C_5H_6N_2S$	126.02517	−0.31	↑
1.45	129.04252	5-oxoproline (pyroglutamic acid)	ESI(−)	$C_5H_7NO_3$	129.04259	0.07	↑
1.19	147.05300	glutamic acid	ESI(−)	$C_5H_9NO_4$	147.05316	0.16	↓
1.23	150.05268	ribulose	ESI(−)	$C_5H_{10}O_5$	150.05282	0.14	↑
1.22	174.11157	arginine	ESI(−)	$C_6H_{14}N_4O_2$	174.11168	0.11	↓
1.20	182.07923	mannitol	ESI(−)	$C_6H_{14}O_6$	182.07904	−0.19	↓
1.27	235.14209	ulvaline	ESI(+)	$C_{10}H_{21}NO_5$	235.14197	−0.12	↑
49.00	282.25607	oleic acid	ESI(−)	$C_{18}H_{34}O_2$	282.25588	−0.19	↑
40.82	300.26619	3-hydroxy-stearic acid	ESI(−)	$C_{18}H_{36}O_3$	300.26645	0.26	↓
29.19	301.29816	sphinganine	ESI(+)	$C_{18}H_{39}NO_2$	301.29810	−0.06	↓
3.20	311.12270	dimethyl guanosine	ESI(+)	$C_{12}H_{17}N_5O_5$	311.12297	0.27	↑
1.48	316.12692	mycosporin glutamicol; 5-carboxylic acid, 1-amide	ESI(+) and ESI(−)	$C_{13}H_{20}N_2O_7$	316.12705	0.13	↓
29.30	317.29239	2-amino-6-methyl-1,3,4-heptadecanetriol	ESI(+)	$C_{18}H_{39}NO_3$	317.29299	0.60	↓
32.57	329.32883	2-amino-1,3-eicosanediol	ESI(+)	$C_{20}H_{43}NO_2$	329.32938	0.55	↓
29.36	345.32362	2-amino-1,3,4-eicosanetriol	ESI(+)	$C_{20}H_{43}NO_3$	345.32429	0.67	↓
1.27	352.22094	unknown 1	ESI(+)	$C_{15}H_{32}N_2O_7$	352.22095	0.01	↑
39.57	434.24330	PA(18:2/0:0)	ESI(−)	$C_{21}H_{39}O_7P$	434.24334	0.04	↑
43.34	436.25894	PA(18:1/0:0)	ESI(−)	$C_{21}H_{41}O_7P$	436.25899	0.05	↑
31.66	451.26996	PE(16:1/0:0)	ESI(+) and ESI(−)	$C_{21}H_{42}NO_7P$	451.26989	−0.07	↓
35.55	453.28541	PE(16:0/0:0)	ESI(−)	$C_{21}H_{44}NO_7P$	453.28554	0.13	↑
35.12	479.30060	PE(18:1/0:0)	ESI(+) and ESI(−)	$C_{23}H_{46}NO_7P$	479.30119	0.59	↓
32.04	493.31640	PC(16:1/0:0)	ESI(+)	$C_{24}H_{48}NO_7P$	493.31684	0.44	↓
34.91	495.33198	PC(16:0/0:0)	ESI(+)	$C_{24}H_{50}NO_7P$	495.33249	0.51	↑
33.17	519.33192	PC(18:2/0:0)	ESI(+)	$C_{26}H_{50}NO_7P$	519.33249	0.57	↓
34.88	521.27549	PS(18:2/0:0)	ESI(−)	$C_{24}H_{44}NO_9P$	521.27537	−0.12	↓
35.82	521.34751	PC(18:1/0:0)	ESI(+)	$C_{26}H_{52}NO_7P$	521.34814	0.63	↓
36.67	523.29086	PS(18:1/0:0)	ESI(+) and ESI(−)	$C_{24}H_{46}NO_9P$	523.29102	0.16	↓
33.37	539.32300	PS(19:0/0:0)	ESI(−)	$C_{25}H_{50}NO_9P$	539.32232	−0.68	↓
36.91	567.35389	PS(21:0/0:0)	ESI(−)	$C_{27}H_{54}NO_9P$	567.35362	−0.27	↓
34.90	596.29639	PI(18:2/0:0)	ESI(−)	$C_{27}H_{49}O_{12}P$	596.29616	−0.23	↓
37.80	598.31236	PI(18:1/0:0)	ESI(−)	$C_{27}H_{51}O_{12}P$	598.31181	−0.55	↓

[a]Abbreviations: PE, phosphatidylethanolamine; PC, phosphotidylcholine; PS, phosphatidyserine; PA, phosphatidic acid; and PI, phosphatidylinositol. [b]Relative metabolite level in conidia of transgenic strains in comparison to the wild-type strain (↑, increase; ↓, decrease).

S plots (Figure 3) showed the most relevant variables affecting differentiation between transgenic and wild-type mycelia and conidia, and the identified biomarkers were summarized in Tables 1 and 2. The high-resolution ESI−TOF−MS data for some metabolites are shown in Figure 4. To test the validity of the OPLS-DA model, we performed a permutation test using the PLS-DA model with the same number of components.[20] Generally, the extrapolated intercept value of $Q^2 < 0.05$ indicates no overfitting in the model. Model validation with the number of permutations equaling 100 generated intercepts of the Q^2 value that were −0.008, −0.027, −0.186, and −0.206, respectively, which showed that the models in this study had good predictability.

3.2. HCA. To visualize the differences of metabolites between mycelia and conidia, a HCA that performs simultaneous clustering of metabolites and samples was used. Before analysis, the data were first mean centered and scaled, then subjected to hierarchical clustering with Spearman's rank correlation and an average linkage clustering method.[21] Figure 5 presented the resulting heat map of 34 metabolites (positive mode; Figure 5A) and 35 metabolites (negative mode; Figure 5B) that were significantly different ($p < 0.01$) from one-way ANOVA. This dendrogram illustrates the arrangements of the clusters of samples and compounds based on similarity of metabolite abundance profiles and biochemical relativity, respectively.[22] Each rectangle represents a metabolite and is colored by its abundance intensities on a normalized scale from −3 (low) to 4 (high). On the *y* axis, mycelia and conidia samples each formed a cluster. In the mycelia and conidia, transformant was clearly separated from the wild-type strain. Metabolites that were biochemically related were generally cluster together on the *x* axis, in positive mode, such as PE(18:1/0:0) (479.30)/PC(18:1/0:0) (521.34), PC(16:1/0:0) (493.31)/PE(16:1/0:0) (451.27), PS(18:1/0:0) (523.29)/PC(18:3/0:0) (517.31), linoleic acid ethyl ester (308.27)/linolenic acid ethyl ester (306.25), beauverolide Ka (630.37)/beauverolide B (543.36), and PE(18:2/0:0) (477.28)/PC(18:2/0:0) (519.33) and in negative mode, such as PE(18:2/0:0) (477.28)/PI(18:2/0:0) (596.29)/PS(18:2/0:0) (521.27), palmitic acid (256.24)/linoleic acid (280.24), 1-hexadecanoyl glucitol (420.30)/mono-9-octadecenoyl glucitol (446.32), beauverolide C (591.36)/beauverolide Ka (630.37)/beauverolide B (543.36), glyoxylate (74.00)/fumarate (116.01), and PE(16:1/0:0) (451.27)/PS(19:0/0:0) (539.32). These results showed good clustering of sample replicates and evident differences between

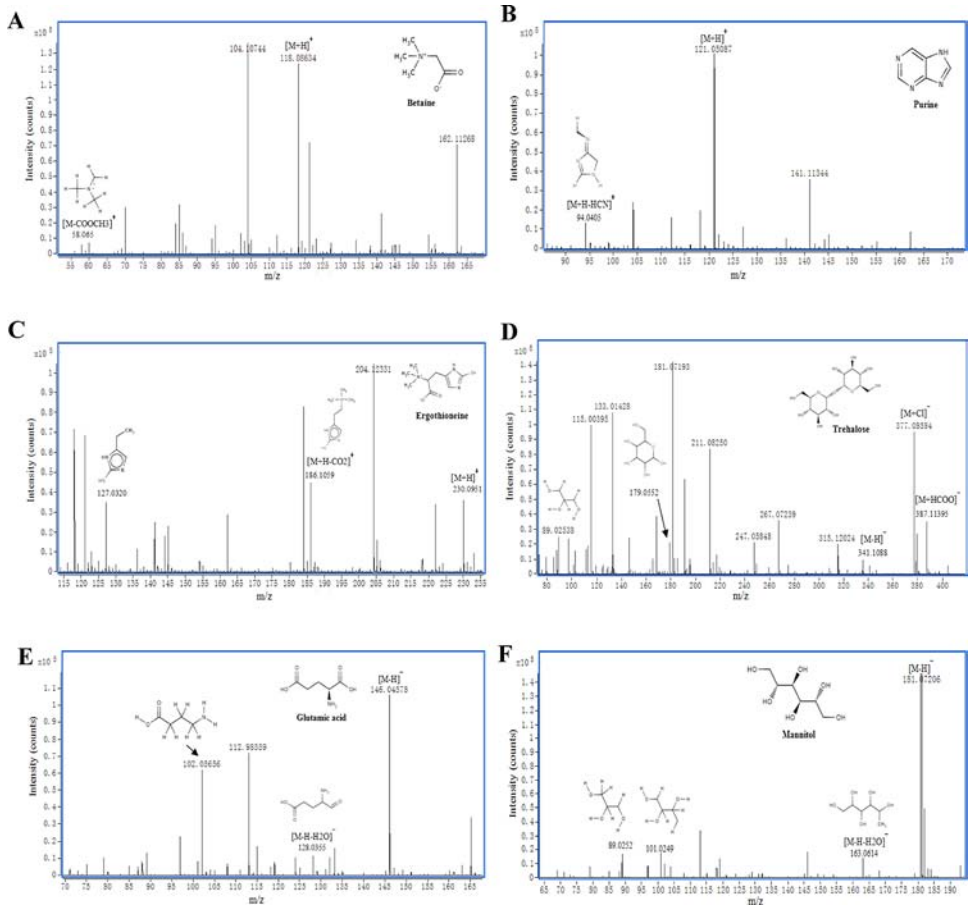

Figure 4. High-resolution mass spectra measured on the ESI−TOF instrument for (A) betaine, (B) purine, and (C) ergothioneine in positive mode and (D) trehalose, (E) glutamic acid, and (F) mannitol in negative mode. The fragment structures are referred to the metlin database.

mycelia and conidia, as well as significant metabolic differences between transgenic and wild-type strains.

3.3. Pathway Analysis. To overall unravel the effects of these metabolites on the metabolic network, the metabolic pathway of some metabolites identified in mycelia and conidia extracts was shown in Figure 6.

As Figure 6 showed, the decrease of glycerophospholipids, esters, carnitine, and fatty acids and the increase of oxylipins, glyoxylate, pyruvic acid, acetylcarnitine, trehalose, and fumarate in transgenic mycelia directly or indirectly indicated that the hydrolysis of lipids and oxidation of fatty acids were promoted.

Oxylipins represent a vast and diverse family of secondary metabolites that originate from the oxidation or further conversion of polyunsaturated fatty acids and a mixture of oxylipins collectively called psi factor.[23] Fungal oxylipins are derived from oleic acid (18:1), linoleic acid (18:2), and linolenic acid (18:3), after the addition of an O_2 molecule to polyunsaturated fatty acids.[24] The decrease of linoleic acid with the increase of 8-hydroxy-linoleic acid and 7,8-dihydroxy-oleic acid in transgenic mycelia (Table 1) indicated that the *aaIT* gene may upregulate the expression of the lipoxygenase gene or the oxylipins may be converted from the non-enzymatic process in response to oxidative stress.[25,26] Oxylipins of pathogenic fungi are important signal factors, which play vital roles in fungal growth, sexual/asexual sporulation, host−fungus crosstalk, host immune defense, and pathogenicity.[23,24,27] Moreover, oxidative stress and oxylipin metabolism are also involved in mycotoxin synthesis.[8,28] Beauverolides are insecticidal cyclodepsipeptides in *B. bassiana*. The increase of beauverolide B, beauverolide C, and beauverolide Ka in the transformant (Table 1) may be related to oxidative stress and/or oxylipin metabolism.

Isocitrate lyase, a key enzyme of the glyoxylate cycle, which mediates the production of glyoxylate from acetyl-CoA and this pathway, is usually induced by excess acetyl-CoA. The higher levels of glyoxylate in transgenic mycelia indicate the enhancement of β-oxidation of fatty acids. It is noteworthy that the glyoxylate cycle has been shown to be required for germination, pathogenesis, and saprobic growth in insect pathogenic fungi.[29] Therefore, it is likely that increased levels of glyoxylate and beauverolides are one reason why the transformant is more toxic than wild isolate.

A decrease of carnitine and an increase of acetylcarnitine and fumarate in transgenic mycelia suggested that parts of acetyl-CoA from β-oxidation of fatty acids enter the mitochondria for tricarboxylic acid (TCA) metabolism, because the carnitine shuttle is essential for acetyl-CoA from peroxisomes to cross mitochondrial membranes, and subsequently, acetyl-CoA was used for the synthesis of AaIT and other metabolites. Furthermore, acetyl units are released from acetylcarnitine in mitochondria, and acetyl-CoA is converted to citrate, which subsequently enters the glyoxylate cycle.

In addition, acetyl-CoA is an activator of pyruvate carboxylase, which catalyzes pyruvate to oxaloacetate and then is converted to phosphopyruvate (PEP), which bypasses the last irreversible reaction of glycolysis. Pyruvic acid and trehalose were increased in transgenic mycelia, implying that gluconeogenesis in engineered mycelia may be stimulated by abundant acetyl-CoA from β-oxidation of fatty acids.

dx.doi.org/10.1021/jf401703b | J. Agric. Food Chem. 2013, 61, 7008−7017

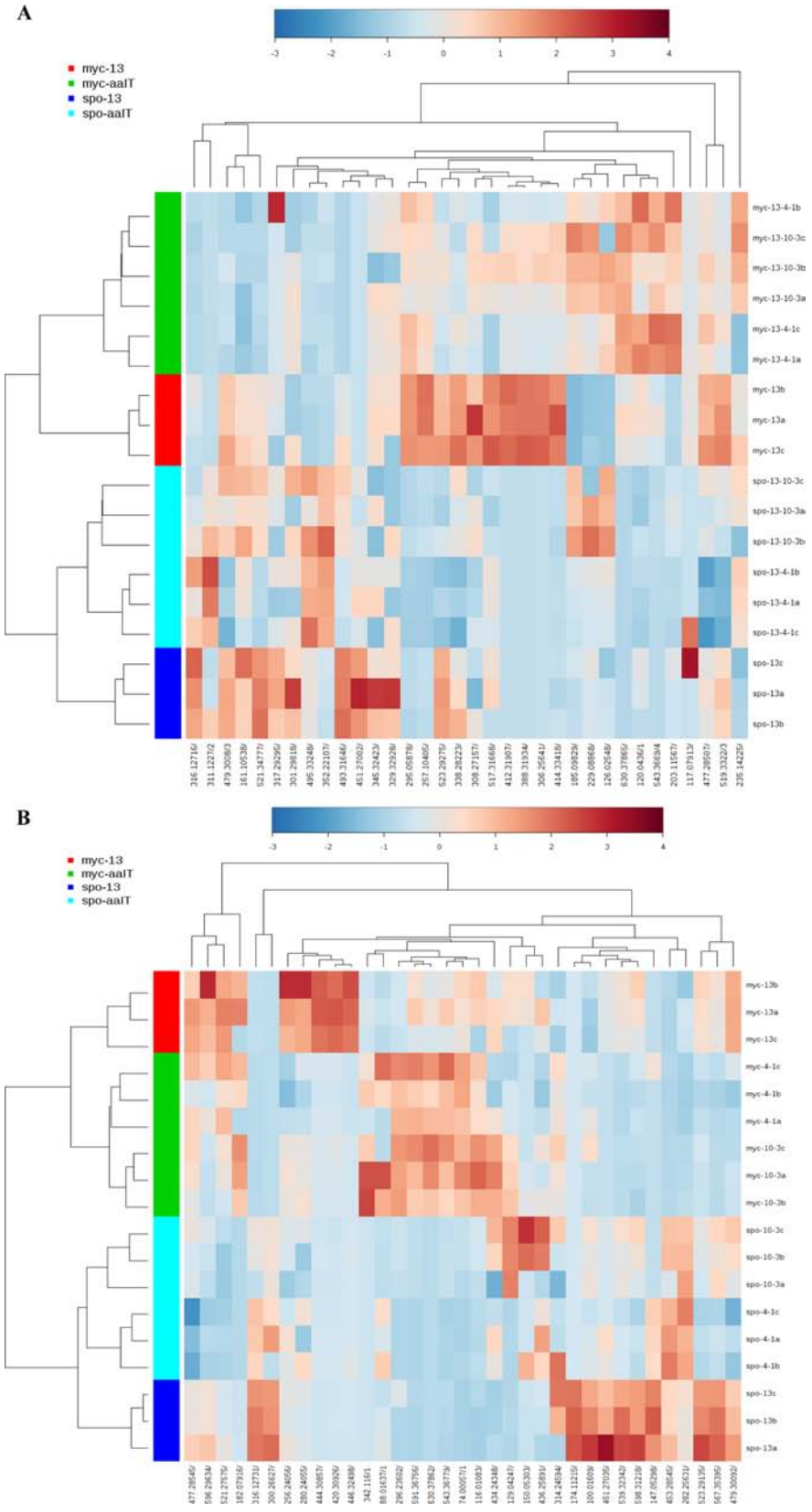

Figure 5. HCA of some metabolites that show statistically significant mycelia and conidia extracts from transgenic and wild-type strains based on MS data in (A) positive mode and (B) negative mode.

The protein kinase AMPK and Snf1 play a central role not only in regulating lipid metabolism (fatty acid oxidation, fatty acid synthesis, and carnitine transport) but also in overall control of energy homeostasis in the eukaryotic and yeast cells, respectively.[30] The alterations of sugars, lipids, and carnitine in the transformant suggested that the energy metabolism of

dx.doi.org/10.1021/jf401703b | J. Agric. Food Chem. 2013, 61, 7008−7017

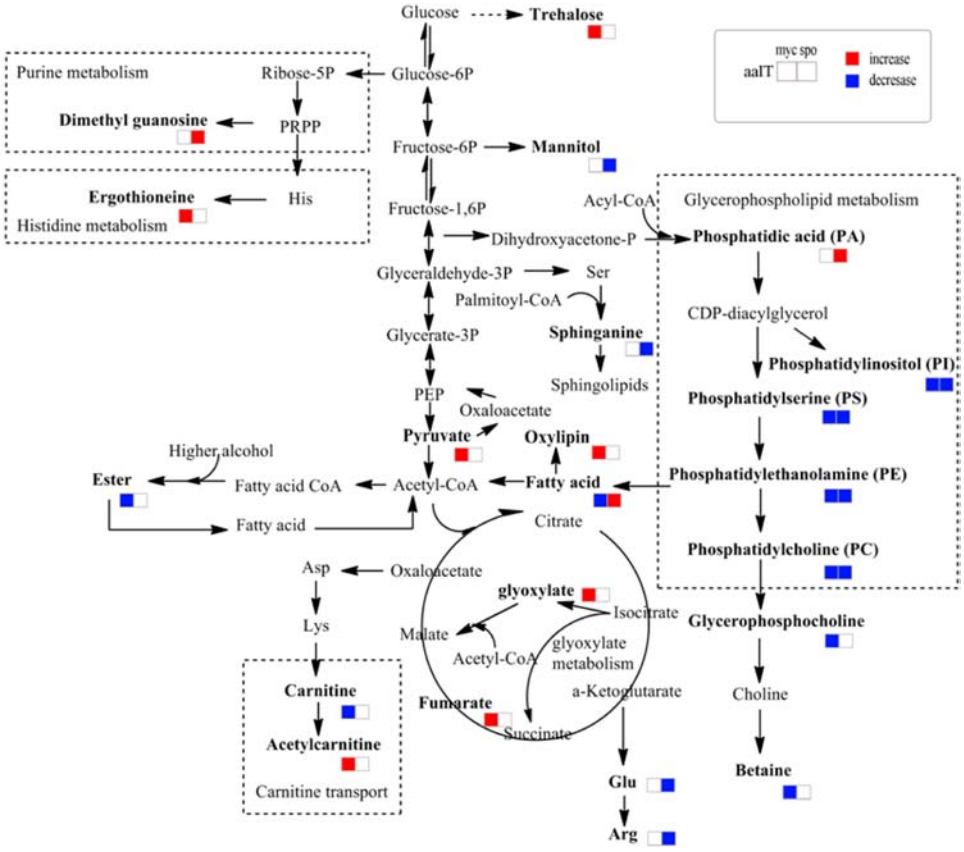

Figure 6. General biosynthetic pathways of some metabolites according to the KEGG database. Mycelium and spore extracts are marked on the left and right of the indicative boxes, respectively. Red and blue denote higher and lower levels of metabolites relative to the wild-type strain, respectively. Abbreviations: PRPP, phosphoribosyl pyrophosphate; PEP, phosphopyruvate.

B. bassiana was interfered by the exogenous gene. Energy metabolism provides a driving force for material metabolism in the biological system. It could be inferred that the global metabolic regulation in transgenic strains is caused by the perturbation of energy metabolism.[31]

Oxidative stress and changes in energy metabolism are due to the introduction of the *aaIT* gene, which is further verified by the increased oxidative stress protectants, such as ergothioneine and trehalose.

Ergothioneine is only produced by fungi and some prokaryotes, and it has a specific role in protecting mitochondrial components, such as DNA, from oxidative damage associated with mitochondrial generation of superoxide[32] and acting as a protectant against UV radiation.[33] Recently, Bello identified an ergothioneine biosynthetic gene *Egt-1* in *Neurospora crass* and demonstrated that ergothioneine enhances conidial survival and protects against peroxide toxicity during conidial germination.[34] Thus, the high levels of ergothioneine in the transformant support the oxidative stress caused by the enhanced oxidative reactions in peroxisomes and mitochondria.

Trehalose, a non-reducing disaccharide, which is usually induced by heat, drying, and oxidative stress and plays roles in stabilizing cell membrane fluidity and protein stability, is widely present in fungi.[35] In this study, fungal cultivations were not subjected to heat and drying treatments; therefore, the higher levels of trehalose in genetic mycelia may be associated with oxidative stress, which is consistent with the increase in ergothioneine. Furthermore, trehalose may play a significant role in fungal pathogenicity. The accumulation of trehalose enhances conidiospore thermotolerance without altering virulence in *Metarhizium acridum*.[36] However, in the study of *Magnaporthe gasea*, trehalose synthesis is required for virulence and it is possible that either trehalose accumulates as an accessory-compatible solute in appressoria or the sugar plays a role in the regulation of appressorium turgor generation.[37]

Relative to mycelia, metabolites related to oxidative stress, such as carnitine, acetylcarnitine, oxylipins, ergothioneine, trehalose, mannitol, etc., are either not significantly changed or even reduced in conidia, which indicated that the oxidative stress is generated in the processes of transcription and translation. There is no significant oxidative stress reaction when the *aaIT* gene is quiescent in conidia. The decrease of phospholipids in conidia may result from the declined import of phospholipids from mycelia in sporulation.

The increased dimethyl guanosine in transgenic conidia might diminish some gene transcription, which would cause slow metabolism and quiescence[38] and lead to improved shelf life of biological insecticide.

A mannitol cycle was first proposed by Hult and Gatenbeck,[39] and this pathway comprises four enzymes: mannitol 1-phosphate dehydrogenase (MPDH), mannitol 1-phosphate phosphatase (MPP), $NADP^+$-mannitol 2-dehydrogenase (MDH), and hexokinase (HX), of which MPDH is the main synthetic enzyme and MDH is the main catabolic enzyme, but the metabolism operating as a cycle has been questioned.[40,41] Mannitol showed a significant decrease in transgenic conidia, indicating that the expression of the *Mpdh* gene may be downregulated by the *aaIT* gene in sporulation. The roles of mannitol vary in different fungi.

dx.doi.org/10.1021/jf401703b | J. Agric. Food Chem. 2013, 61, 7008−7017

Mannitol might act as a scavenger of reactive oxygen species in plant pathogen *Uromyces fabae*.[42] Wheat pathogen *Stagonospora nodorum* mannitol gene mutants are unable to sporulate on host plants, but their pathogenicity is not compromised.[43,44] In contrast, mannitol biosynthesis is required for pathogenesis of *Alternaria alternata* on tobacco but is not required for spore germination.[45] Therefore, the lower levels of mannitol in transgenic conidia may have an important impact on environment adaptability, sporulation, and virulence.

Sphingosine is a signaling lipid and may be involved in insect−fungi recognition. A C_{14}-sphingosine that can recognize the receptors on conidia and induce the germination of *Nomuraea rileyi* was isolated from the silkworm pupae.[46] Sphinganine is the biosynthetic precursor of sphingosines and sphingolipids, and its decrease in transgenic conidia may affect fungal signaling.

We have investigated mycelia and conidia extracts of transgenic and wild-type *B. bassiana* using a LC−MS-based metabolomic approach. The results of PCA have displayed clear differences of mycelia and conidia between transgenic and wild-type strains, implying that the introduction of the *aaIT* gene has strongly influenced the metabolism of *B. bassiana*. Many significant biomarkers in mycelia and conidia can be identified by OPLS-DA. HCA further corroborates significant metabolic differences between transgenic and wild-type strains.

Pathway analysis has shown that many changed metabolites in mycelia are correlated with oxidative stress and energy metabolism. More specifically, (1) a decrease of fatty acids and an increase of oxylipins are due to β-oxidation of fatty acids and the reaction of adding an O_2 molecule to fatty acids, respectively; (2) the biosynthesis of glyoxylate is facilitated by isocitrate lyase, which may be stimulated by acetyl-CoA generated from β-oxidation of fatty acids; (3) carnitine shuttle helps acetyl-CoA cross mitochondrial membranes to enter the TCA cycle for the synthesis of proteins (AaIT, beauverolides, etc.) and other metabolites; and (4) gluconeogenesis metabolism accelerated for the pyruvate carboxylase may be induced by excessive acetyl-CoA. These changes lead to enhanced oxidative reactions in cells. Correspondingly, some antioxidant metabolites, such as ergothioneine and trehalose, show higher levels in transgenic mycelia, suggesting that fungal cells are under oxidative stress and cellular protective response has been induced by oxidative stress.

In contrast to mycelia, although glycerophospholipids are decreased in engineered conidia, other compounds related to oxidative stress, such as carnitine, oxylipins, ergothioneine, trehalose, mannitol, etc., are either not significantly changed or even reduced in conidia. This difference indicates that the oxidative stress is generated in the processes of transcription and translation; therefore, there is no significant oxidative stress reaction when the *aaIT* gene is quiescent in conidia.

AUTHOR INFORMATION

Corresponding Author

*Telephone/Fax: +86-551-5786887. E-mail: hufenglin@hotmail.com.

Funding

This work was funded by the Ministry of Science and Technology of Anhui Province (Grants 11040606M69 and KJ2012A107) and the National Natural Science Foundation of China (Grant 30871676).

Notes

The authors declare no competing financial interest.

REFERENCES

(1) St. Leger, R. J.; Wang, C. S. Genetic engineering of fungal biocontrol agents to achieve greater efficacy against insect pests. *Appl. Microbiol. Biotechnol.* **2010**, *85*, 901−907.

(2) de Faria, M. R.; Wraight, S. P. Mycoinsecticides and mycoacaricides: A comprehensive list with worldwide coverage and international classification of formulation types. *Biol. Control* **2007**, *43*, 237−256.

(3) Pava-Ripoll, M.; Posada, F. J.; Momen, B.; Wang, C.; Leger, R. S. Increased pathogenicity against coffee berry borer, *Hypothenemus hampei* (Coleoptera: Curculionidae) by *Metarhizium anisopliae* expressing the scorpion toxin (AaIT) gene. *J. Invertebr. Pathol.* **2008**, *99*, 220−226.

(4) Wang, C.; St. Leger, R. J. A scorpion neurotoxin increases the potency of a fungal insecticide. *Nat. Biotechnol.* **2007**, *25*, 1455−1456.

(5) Zlotkin, E.; Fishman, Y.; Elazar, M. AaIT: From neurotoxin to insecticide. *Biochimie* **2000**, *82*, 869−881.

(6) Ji, S. J.; Liu, F.; Li, E. Q.; Zhu, Y. X. Recombinant scorpion insectotoxin AaIT kills specifically insect cells but not human cells. *Cell Res.* **2002**, *12*, 143−150.

(7) Lu, D. D.; Pava-Ripoll, M.; Li, Z. Z.; Wang, C. S. Insecticidal evaluation of *Beauveria bassiana* engineered to express a scorpion neurotoxin and a cuticle degrading protease. *Appl. Microbiol. Biotechnol.* **2008**, *81*, 515−522.

(8) Trienens, M.; Rohlfs, M. Insect−fungus interference competition—The potential role of global secondary metabolite regulation, pathway-specific mycotoxin expression and formation of oxylipins. *Fungal Ecol.* **2012**, *5*, 191−199.

(9) Chen, F. F.; Zhang, J. T.; Song, X. S.; Yang, J.; Li, H. P.; Tang, H. R.; Liao, Y. C. Combined metabonomic and quantitative real-time PCR analyses reveal systems metabolic changes of *Fusarium graminearum* induced by Tri5 gene deletion. *J. Proteome Res.* **2011**, *10*, 2273−2285.

(10) Leon, C.; Rodriguez-Meizoso, I.; Lucio, M.; Garcia-Canas, V.; Ibanez, E.; Schmitt-Kopplin, P.; Cifuentes, A. Metabolomics of transgenic maize combining Fourier transform-ion cyclotron resonance−mass spectrometry, capillary electrophoresis−mass spectrometry and pressurized liquid extraction. *J. Chromatogr., A* **2009**, *1216*, 7314−7323.

(11) Hanhineva, K.; Kokko, H.; Siljanen, H.; Rogachev, I.; Aharoni, A.; Karenlampi, S. O. Stilbene synthase gene transfer caused alterations in the phenylpropanoid metabolism of transgenic strawberry (*Fragaria* × *ananassa*). *J. Exp. Bot.* **2009**, *60*, 2093−2106.

(12) Manetti, C.; Bianchetti, C.; Casciani, L.; Castro, C.; Di Cocco, M. E.; Miccheli, A.; Motto, M.; Conti, F. A metabonomic study of transgenic maize (Zea mays) seeds revealed variations in osmolytes and branched amino acids. *J. Exp. Bot.* **2006**, *57*, 2613−2625.

(13) Xia, J. G.; Wishart, D. S. Web-based inference of biological patterns, functions and pathways from metabolomic data using MetaboAnalyst. *Nat. Protoc.* **2011**, *6*, 743−760.

(14) Xia, J. G.; Psychogios, N.; Young, N.; Wishart, D. S. MetaboAnalyst: A web server for metabolomic data analysis and interpretation. *Nucleic Acids Res.* **2009**, *37*, W652−W660.

(15) Danielsson, R.; Allard, E.; Sjöberg, P. J. R.; Bergquist, J. Exploring liquid chromatography−mass spectrometry fingerprints of urine samples from patients with prostate or urinary bladder cancer. *Chemom. Intell. Lab. Syst.* **2011**, *108*, 33−48.

(16) Zhao, X. J.; Fritsche, J.; Wang, J. S.; Chen, J.; Rittig, K.; Schmitt-Kopplin, P.; Fritsche, A.; Haring, H. U.; Schleicher, E. D.; Xu, G. W.; Lehmann, R. Metabonomic fingerprints of fasting plasma and spot urine reveal human pre-diabetic metabolic traits. *Metabolomics* **2010**, *6*, 362−374.

(17) Okuda, S.; Yamada, T.; Hamajima, M.; Itoh, M.; Katayama, T.; Bork, P.; Goto, S.; Kanehisa, M. KEGG Atlas mapping for global analysis of metabolic pathways. *Nucleic Acids Res.* **2008**, *36*, W423.

(18) Ametaj, B. N.; Zebeli, Q.; Saleem, F.; Psychogios, N.; Lewis, M. J.; Dunn, S. M.; Xia, J. G.; Wishart, D. S. Metabolomics reveals unhealthy alterations in rumen metabolism with increased proportion of cereal grain in the diet of dairy cows. *Metabolomics* **2010**, *6*, 583−594.
(19) Abdel-Farid, I. B.; Jahangir, M.; van den Hondel, C.; Kim, H. K.; Choi, Y. H.; Verpoorte, R. Fungal infection-induced metabolites in *Brassica rapa*. *Plant Sci.* **2009**, *176*, 608−615.
(20) Lee, J. E.; Lee, B. J.; Chung, J. O.; Hwang, J. A.; Lee, S. J.; Lee, C. H.; Hong, Y. S. Geographical and climatic dependencies of green tea (*Camellia sinensis*) metabolites: A ^{1}H NMR-based metabolomics study. *J. Agric. Food Chem.* **2010**, *58*, 10582−10589.
(21) Sun, J. C.; Schnackenberg, L. K.; Pence, L.; Bhattacharyya, S.; Doerge, D. R.; Bowyer, J. F.; Beger, R. D. Metabolomic analysis of urine from rats chronically dosed with acrylamide using NMR and LC/MS. *Metabolomics* **2010**, *6*, 550−563.
(22) Denkert, C.; Budczies, J.; Kind, T.; Weichert, W.; Tablack, P.; Sehouli, J.; Niesporek, S.; Konsgen, D.; Dietel, M.; Fiehn, O. Mass spectrometry-based metabolic profiling reveals different metabolite patterns in invasive ovarian carcinomas and ovarian borderline tumors. *Cancer Res.* **2006**, *66*, 10795−10804.
(23) Tsitsigiannis, D. I.; Keller, N. P. Oxylipins as developmental and host−fungal communication signals. *Trends Microbiol.* **2007**, *15*, 109−118.
(24) Singh, A.; Del Poeta, M. Lipid signalling in pathogenic fungi. *Cell Microbiol.* **2011**, *13*, 177−185.
(25) Mueller, M. J. Archetype signals in plants: The phytoprostanes. *Curr. Opin. Plant Biol.* **2004**, *7*, 441−448.
(26) Fam, S. S.; Morrow, J. D. The isoprostanes: Unique products of arachidonic acid oxidation—A review. *Curr. Med. Chem.* **2003**, *10*, 1723−1740.
(27) Erb-Downward, J. R.; Huffnagle, G. B. Role of oxylipins and other lipid mediators in fungal pathogenesis. *Future Microbiol.* **2006**, *1*, 219−227.
(28) Reverberi, M.; Gazzetti, K.; Punelli, F.; Scarpari, M.; Zjalic, S.; Ricelli, A.; Fabbri, A. A.; Fanelli, C. Aoyap1 regulates OTA synthesis by controlling cell redox balance in *Aspergillus ochraceus*. *Appl. Microbiol. Biot.* **2012**, *95*, 1293−1304.
(29) Padilla-Guerrero, I. E.; Barelli, L.; Gonzalez-Hernandez, G. A.; Torres-Guzman, J. C.; Bidochka, M. J. Flexible metabolism in *Metarhizium anisopliae* and *Beauveria bassiana*: Role of the glyoxylate cycle during insect pathogenesis. *Microbiology* **2011**, *157*, 199−208.
(30) Nielsen, J. Systems biology of lipid metabolism: From yeast to human. *FEBS Lett.* **2009**, *583*, 3905−3913.
(31) Swann, J. R.; Tuohy, K. M.; Lindfors, P.; Brown, D. T.; Gibson, G. R.; Wilson, I. D.; Sidaway, J.; Nicholson, J. K.; Holmes, E. Variation in antibiotic-induced microbial recolonization impacts on the host metabolic phenotypes of rats. *J. Proteome Res.* **2011**, *10*, 3590−3603.
(32) Paul, B. D.; Snyder, S. H. The unusual amino acid L-ergothioneine is a physiologic cytoprotectant. *Cell Death Differ.* **2010**, *17*, 1134−1140.
(33) Cheah, I. K.; Halliwell, B. Ergothioneine; antioxidant potential, physiological function and role in disease. *Biochim. Biophys. Acta, Mol. Basis Dis.* **2012**, *1822*, 784−793.
(34) Bello, M. H.; Barrera-Perez, V.; Morin, D.; Epstein, L. The *Neurospora crassa* mutant NcΔEgt-1 identifies an ergothioneine biosynthetic gene and demonstrates that ergothioneine enhances conidial survival and protects against peroxide toxicity during conidial germination. *Fungal Genet. Biol.* **2012**, *49*, 160−172.
(35) Elbein, A. D.; Pan, Y.; Pastuszak, I.; Carroll, D. New insights on trehalose: A multifunctional molecule. *Glycobiology* **2003**, *13*, 17R−27R.
(36) Leng, Y. J.; Peng, G. X.; Cao, Y. Q.; Xia, Y. X. Genetically altering the expression of neutral trehalase gene affects conidiospore thermotolerance of the entomopathogenic fungus *Metarhizium acridum*. *BMC Microbiol.* **2011**, *11*, 32.
(37) Wang, Z. Y.; Jenkinson, J. M.; Holcombe, L. J.; Soanes, D. M.; Veneault-Fourrey, C.; Bhambra, G. K.; Talbot, N. J. The molecular biology of appressorium turgor generation by the rice blast fungus *Magnaporthe gasea*. *Biochem. Soc. Trans.* **2005**, *33*, 384−388.
(38) Pluskal, T.; Hayashi, T.; Saitoh, S.; Fujisawa, A.; Yanagida, M. Specific biomarkers for stochastic division patterns and starvation-induced quiescence under limited glucose levels in fission yeast. *FEBS J.* **2011**, *278*, 1299−1315.
(39) Hult, K.; Gatenbeck, S. Production of NADPH in the mannitol cycle and its relation to polyketide formation in *Alternaria alternata*. *Eur. J. Biochem.* **1978**, *88*, 607−612.
(40) Solomon, P. S.; Waters, O. D. C.; Oliver, R. P. Decoding the mannitol enigma in filamentous fungi. *Trends Microbiol.* **2007**, *15*, 257−262.
(41) Velez, H.; Glassbrook, N. J.; Daub, M. E. Mannitol metabolism in the phytopathogenic fungus *Alternaria alternata*. *Fungal Genet. Biol.* **2007**, *44*, 258−268.
(42) Voegele, R. T.; Hahn, M.; Lohaus, G.; Link, T.; Heiser, I.; Mendgen, K. Possible roles for mannitol and mannitol dehydrogenase in the biotrophic plant pathogen *Uromyces fabae*. *Plant Physiol.* **2005**, *137*, 190−198.
(43) Solomon, P. S.; Waters, O. D. C.; Jorgens, C. I.; Lowe, R. G. T.; Rechberger, J.; Trengove, R. D.; Oliver, R. P. Mannitol is required for asexual sporulation in the wheat pathogen *Stagonospora nodorum* (glume blotch). *Biochem. J.* **2006**, *399*, 231−239.
(44) Solomon, P. S.; Tan, K. C.; Oliver, R. P. Mannitol 1-phosphate metabolism is required for sporulation in planta of the wheat pathogen *Stagonospora nodorum*. *Mol. Plant-Microbe Interact.* **2005**, *18*, 110−115.
(45) Veleaz, H.; Glassbrook, N. J.; Daub, M. E. Mannitol biosynthesis is required for plant pathogenicity by *Alternaria alternata*. *FEMS Microbiol. Lett.* **2008**, *285*, 122−129.
(46) Noda, T.; Ono, M.; Iimure, K.; Araki, T. Characterization of a germination-accelerating factor from the silkworm (*Bombyx mori* Linnaeus) of entomopathogenic fungus *Nomuraea rileyi* (Farlow) Samson. *Biosci., Biotechnol., Biochem.* **2010**, *74*, 1226−1230.